Published online July 1, 2004

Nucleic Acids Research, 2004, Vol. 32, No. 11 ***3493–3502***
DOI: 10.1093/nar/gkh668

Binding of phage Φ29 architectural protein p6 to the viral genome: evidence for topological restriction of the phage linear DNA

Víctor González-Huici, Martín Alcorlo, Margarita Salas* and José M. Hermoso

Instituto de Biología Molecular 'Eladio Viñuela' (CSIC), Centro de Biología Molecular 'Severo Ochoa' (CSIC-UAM), Universidad Autónoma, Canto Blanco, 28049 Madrid, Spain

Received April 8, 2004; Revised May 18, 2004; Accepted June 6, 2004

ABSTRACT

Bacillus subtilis **phage Φ29 protein p6 is required for DNA replication and promotes the switch from early to late transcription. *In vivo* it binds all along the viral linear DNA, which suggests a global role as an architectural protein; in contrast, binding to bacterial DNA is negligible. This specificity could be due to the p6 binding preference for less negatively supercoiled DNA, as is presumably the case with viral (with respect to bacterial) DNA. Here we demonstrate that p6 binding to Φ29 DNA is greatly increased when negative supercoiling is decreased by novobiocin; in addition, gyrase is required for DNA replication. This indicates that, although non-covalently closed, the viral genome is topologically constrained *in vivo*. We also show that the p6 binding to different Φ29 DNA regions is modulated by the structural properties of their nucleotide sequences. The higher affinity for DNA ends is possibly related to the presence of sequences in which their bendability properties favor the formation of the p6–DNA complex, whereas the lower affinity for the transcription control region is most probably due to the presence of a rigid intrinsic DNA curvature.**

INTRODUCTION

From higher eukaryotes to bacteria, non-sequence-specific, DNA binding proteins assume the essential function of packaging and organizing the genome inside the cell. These architectural proteins, far from merely compacting DNA to fit it into the cell or nuclear compartment, control DNA structure, topology and accessibility to proteins to regulate such functions as replication, transcription, recombination, repair and segregation. In Eukarya, histones compact and scaffold chromosomes into a chromatin fiber formed by nucleosomes. The structure of chromatin can be modulated by covalent modification of histones, DNA methylation or the interaction with non-histone proteins such as heterochromatin protein 1 and high mobility group (HMG) proteins (1,2). The HMG group is a family of proteins that seems to be involved in the manipulation of nucleoprotein complexes and in chromatin structure maintenance (3,4). On the other hand, SMC proteins, condensins and cohesins are ATPases that form complexes with other proteins to perform an essential role in chromosome condensation, cohesion, transcriptional control, recombination and repair (5,6).

In Eubacteria, it has been proposed that a heterogeneous group of proteins, denominated 'histone-like' according to a functional criterion, is responsible for genome organization [for reviews see (7,8)]. In *Escherichia coli* the most abundant ones are HU, Fis, H-NS, IHF, Dps and StpA (9); they are mostly non-sequence-specific and it is proposed that they are distributed along the entire nucleoid (10). *E.coli* contains a protein, MukB, with a structure similar to that of SMC (11). In *Bacillus subtilis*, 'histone-like' proteins such as HBsu (12), LrpC (13) and L24 (14) have been described. A single SMC protein is also found in *B.subtilis*. Both SMC and MukB are essential for chromosome condensation, supercoiling and correct partitioning (15). Recently, two highly conserved prokaryotic proteins, ScpA and ScpB, have been shown to interact with SMC, performing similar functions (16,17).

The *B.subtilis* phage Φ29-encoded protein p6 is essential for DNA replication *in vivo* (18,19), activating *in vitro* the initiation step (20,21). It is also involved in transcription control, repressing C2 early promoter at the DNA right end (22–24) and, together with the viral regulatory protein p4, repressing early promoters A2b/A2c and activating late promoter A3 (25). *In vitro* both the stimulation of initiation of DNA replication and the repression of early promoters require the formation of a protein p6–DNA nucleoprotein complex, in which the DNA forms a right-handed toroidal superhelix around a multimeric protein core (26,27). However, *in vivo* protein p6 binds to most, if not all, of the Φ29 DNA (28), so its functions in replication and transcription could be outcomes of a more global role as a histone-like protein which participates in organization and compaction of the viral genome. In fact, its small size and abundance in infected cells [∼700 000 copies per cell, (29)] are features expected for a protein with such an architectural role. Like p6, the four major histone-like proteins of *E.coli*, HU, IHF, Fis and H-NS are also involved in transcription control (30,31), particularly H-NS, which controls the expression of at least 5% of the genes in the cell (32,33). In addition, the ability to stimulate initiation

*To whom correspondence should be addressed. Tel: +34 91 4978435; Fax: +34 91 4978490; Email: msalas@cbm.uam.es

of replication has been described for proteins HU and IHF (7,34,35).

Protein p6 binding is inversely proportional to the degree of negative supercoiling of DNA, as shown *in vivo* and *in vitro* (28), in agreement with its *in vitro* ability to restrain positive supercoiling [ΔL_k of +0.1 per protein p6 dimer, (27)]. *In vivo*, protein p6 binding to all the Φ29 DNA regions analyzed was much higher than binding to a negatively supercoiled plasmid (28), most probably indicating that the Φ29 genome has a lower negative superhelicity than the plasmid. In fact, Φ29 DNA has a terminal protein and therefore is not covalently closed, but this does not necessarily mean that it is relaxed, as attachment of the terminal proteins to the membrane could topologically restrain the genome. Thus, the first question we address in this paper is whether the Φ29 genome is topologically constrained *in vivo*. If this is so, we could expect improved p6 binding to DNA after novobiocin treatment; in addition, DNA replication would be impaired by using the gyrase inhibitors novobiocin and nalidixic acid. The second question was to find out the reason for the differences in protein p6 binding to the different Φ29 DNA regions, namely the enhanced affinity for both DNA ends and the particularly low affinity for the region comprising the main promoters A2b-A2c-A3 (28). We considered two main hypotheses: the presence of independent topological domains, as found in bacterial genomes (36,37), and preferential binding to certain nucleotide sequences (38). For this we have studied p6 binding to isolated Φ29 DNA regions: *in vivo* by crosslinking and chromatin immunoprecipitation (X-ChIP) and *in vitro* by fluorescence quenching.

We conclude that Φ29 DNA is topologically constrained *in vivo*, a feature that may be essential for the regulation of p6 functions. In addition, the observed *in vivo* differences in p6 affinity among Φ29 DNA regions seem to depend on structural features of nucleotide sequences rather than on the existence of independent topological domains.

MATERIALS AND METHODS

Bacteria, plasmids and phages

B.subtilis 110NA (trpC2, spoOA3, su^-) (39) containing the pUB110 derivative pPR55ow6 (40) and *E.coli* λ lysogen κ-12Δtrp (λN^-cI857ΔH1) (K-12ΔH1Δtrp) containing plasmid pRP8, a pBR322 derivative with the Φ29 gene *6* under the control of λ thermosensitive promoter P_L (20), were used. Plasmid pACYC184 was obtained from Mobitech. Bacteria were grown in Luria–Bertani (LB) medium supplemented with 5 mM $MgSO_4$. *E.coli* harboring pRP8 and pACYC184 plasmids was grown in the presence of 100 μg/ml ampicillin and 34 μg/ml chloramphenicol. Phage Φ29 *sus14* (1242), a delayed lysis mutant (41), was used for the infections.

Enzymes, drugs and reactives

Micrococcal nuclease was from Amersham Pharmacia Biotech and proteinase K from Boehringer Mannheim. Protein A-Sepharose CL-4B, lysozyme, RNase A, chloramphenicol, novobiocin and nalidixic acid were from Sigma. Formaldehyde at 37% was purchased from Calbiochem. Restriction enzymes, Klenow fragment, Vent DNA polymerase, polynucleotide kinase and T4 ligase were from New England Biolabs. Alkaline phosphatase was from Promega.

DNAs and oligonucleotides

Proteinase-K-digested Φ29 DNA was obtained as described in (42). DNA fragments for fluorescence analyses were obtained by PCR in a Light-Cycler apparatus (Roche). A pre-heating step of 20 min at 95°C was performed to activate the polymerase, followed by 30 amplification cycles. The PCR conditions and the Φ29 DNA coordinates of the fragments are shown in Table 1. The sequences of the primers are available upon request.

Cloning of Φ29 DNA fragments in p6-producing *E.coli* cells

Recombinant plasmids derived from pACYC184 were constructed by inserting into the EcoRV site the DNA fragments named L, R, C and AO. Blunt-ended Φ29 terminal fragments (L, R) were obtained by digestion of plasmids pL259 and pR259, respectively (43), with DraI and EcoRV. The $(24)_{12}$ concatemer (C) was obtained from plasmid p$(24)_{12}$, a pUC19 derivative (27), digested with BamHI and HindIII and filled in with Klenow fragment to generate blunt ends. The fragment of *E.coli* nadB gene for L-aspartate oxidase (AO) was obtained by PCR, using Vent DNA polymerase. The fragments were then phosphorylated and purified from agarose gel using the Quiaquick Gel Extraction Kit (Qiagen). Plasmid pACYC184 was digested with EcoRV, dephosphorylated, purified from agarose gel and ligated to each of the four fragments. *E.coli* NF1 cells were transformed by electroporation and recombinants analyzed by restriction with BamHI and HindIII, followed by sequencing of the insert.

Crosslinking, immunoprecipitation and DNA amplification

X-ChIP was performed essentially as described in (44), with slight modifications. Bacteria were grown at 30°C up to 10^8 cells/ml. *B.subtilis* was infected with Φ29 *sus14* (1242) at a multiplicity of infection of 10. *E.coli* harboring plasmid pRP8 was incubated at 37°C for 15 min to induce p6 synthesis. Culture samples, 20 ml each, were treated directly with 1% formaldehyde, together with 10 mM sodium phosphate, pH 7.2. After 5 min at room temperature without shaking, reactions were stopped by addition of 125 mM glycine.

Table 1. DNA fragments used in this work

Fragment name	Φ29 DNA coordinates	PCR conditions Melting	Hybridization	Elongation
L	1–259	15 s, 95°C	5 s, 53°C	15 s, 72°C
4.9	4752–5087	15 s, 95°C	10 s, 48°C	60 s, 72°C
5.1	4895–5257	15 s, 95°C	10 s, 48°C	60 s, 72°C
5.3	5134–5462	15 s, 95°C	10 s, 48°C	60 s, 72°C
7.4	7255–7528	15 s, 95°C	10 s, 51°C	30 s, 72°C
9.7	9507–9820	15 s, 95°C	10 s, 51°C	30 s, 72°C
11.7	11567–11778	15 s, 95°C	5 s, 53°C	15 s, 72°C
R	18988–19285	15 s, 95°C	5 s, 50°C	40 s, 72°C
C	n.a.	15 s, 95°C	10 s, 58°C	40 s, 72°C

PCR amplification conditions and coordinates from Φ29 DNA left end of the DNA fragments used for cloning (Figure 3) and/or fluorescence quenching assays (Figures 4 and 5). n.a.: Not applicable.

Cells were harvested by centrifugation, washed twice with PBS buffer, resuspended in 1 ml of buffer A (10 mM Tris–HCl, pH 8.0, 50 mM NaCl, 10 mM EDTA) with 3 mg/ml lysozyme, incubated for 30 min at 37°C and lysed by addition of 1 ml of 2× IP buffer (100 mM Tris–HCl, pH 7.0, 300 mM NaCl, 2% Triton X-100) with 0.1% SDS. Then, 0.05 U of micrococcal nuclease, together with 13 mM $CaCl_2$, were added. After 10 min at 37°C, digestion was stopped with 20 mM EDTA, and DNA was sheared to an average size of 750 bp by sonication, eliminating cell debris by centrifugation. One-twentieth of each sample was kept for total DNA analysis and the remainder was divided into two equal aliquots to perform immunoprecipitation overnight at 4°C, with 20 µl of either αp6 polyclonal antibodies or pre-immune serum, followed by incubation for 2.5 h at 4°C with 120 µl of a 25% protein A-Sepharose slurry. Complexes were collected by centrifugation and washed twice with 1× IP-0.1% SDS buffer, three times with 1× IP buffer and twice with TE buffer. The slurry was resuspended in 150 µl of TE buffer containing 1% SDS to disrupt immune complexes. Total DNA samples (*T*) were also brought to a total volume of 150 µl TE containing 1% SDS. All samples were incubated overnight at 65°C with shaking to reverse crosslinks. Slurry was removed by centrifugation and the supernatant transferred to a fresh tube. DNA was purified by phenol:chloroform extraction, ethanol-precipitated and finally resuspended in water.

Analysis of DNA samples was performed by real-time PCR in a Light-Cycler instrument using a 'Light Cycler-FastStart DNA Master SYBR Green I' hot-start reaction mix (Roche). The data were interpolated to a standard curve constructed with known amounts of purified, full-length, Φ29 or plasmid DNA. The results were expressed as picograms of Φ29 or plasmid DNA per milliliter of culture. Protein p6 binding was expressed as the immunoprecipitation coefficient (IC); $IC = [(\alpha p6 - pi)/T] \times 10^6$, where *T* is total DNA, αp6 the DNA immunoprecipitated with serum against p6 and pi the DNA immunoprecipitated with pre-immune serum.

In the case of infected *B.subtilis* the amplification conditions for Φ29 DNA were those described for obtaining DNA fragments for fluorescence assays (see above). Fragment L corresponds to region Φ1, 5.1 to region Φ2, 7.4 to region Φ3, 9.7 to region Φ4, 11.7 to region Φ5 and R to region Φ6. For *E.coli* cells containing pACYC184 derivatives, regions P1 (positions 1612–1711, without considering the length of the insert) and P2 (3607–3979) were amplified. The PCR was performed as for Φ29 DNA, with a hybridization step of 10 s at 58°C for P1 and 52°C for P2, and an elongation of 40 s at 72°C for both. In all cases, a melting analysis was performed by continuous fluorescence measurement from 65 to 95°C, to ensure the presence of a single specific amplification product.

Fluorescence measurements

Fluorescence measurements were performed in a Varian Cary Eclipse spectrofluorometer and monitored in a 2 mm path length cell, at a temperature of 15°C. The tryptophan residue of protein p6 was excited at a wavelength of 290 nm and fluorescence measured at 350 nm.

To determine the effective binding constant ($K_{eff} = K_\omega$) of protein p6 to the different DNA fragments, direct titration experiments were performed (45,46). Protein p6 was added to DNA (20 µM) in a buffer of 50 mM Tris–HCl, pH 7.5, 10 mM $MgCl_2$, measuring fluorescence after mixing the sample by gentle shaking and incubating for 15–45 s. To calculate the K_{eff}, we carried out a fitting procedure based on previously published expressions (45) and on the theory of McGhee and von Hippel (47), for the binding of proteins to polynucleotides. The fitting procedure was started by fixing the values of Q_{max}, f_A and the binding site size (*n*) and setting *K* and ω as the fitting parameters, and continued by an iteration algorithm designed in our laboratory (48). We also performed a graphical approximation to K_{eff} as described in (46). In a plot of the saturation fraction against $[p6]_{free}$, assuming that $\omega \gg n$, the value of $[p6]_{free}$ corresponding to half saturation yields $1/K_\omega$ (47,49).

RESULTS

The Φ29 genome is topologically constrained *in vivo*

Phage Φ29 protein p6 binds all along Φ29 DNA *in vivo* with a much higher affinity than for plasmid DNA. This could be due to a lower negative superhelicity of Φ29 DNA, as negative supercoiling impairs p6 binding to DNA (28). Although phage Φ29 DNA has a terminal protein, and therefore is not covalently closed, it could be topologically constrained, as described for bacteriophage T4 (37). To study this possibility, we used X-ChIP (50) and real-time PCR to measure p6 binding *in vivo* to six regions scattered throughout the Φ29 genome (Φ1 to Φ6, see Figure 1A) in the absence or presence of novobiocin. Novobiocin produces a loss of negative supercoiling (51), so if Φ29 DNA were topologically constrained, we would expect an increase of p6 binding. As a control, we used nalidixic acid, which also inhibits gyrase but has no topological effects. It is important to note that the analyzed regions include a much wider region (~1.2 kb, in gray) than the PCR-amplified sequences (~300 bp, in black), as the average size of the DNA fragments after sonication is ~750 bp. Figure 1B shows that protein p6 binding, expressed as the immunoprecipitation coefficient (IC, see Materials and Methods), increases 23- to -35-fold with respect to the control upon addition of novobiocin, except in the case of region Φ2, where the increase is about 8-fold. Although binding to all Φ29 DNA regions is dramatically increased by novobiocin, the differences observed among them in the absence of inhibitors are qualitatively conserved. Nalidixic acid produced essentially no change in the IC values. These results suggest that Φ29 DNA, although not covalently closed, is topologically constrained *in vivo*.

To further investigate this issue we studied the effect of gyrase inhibitors in Φ29 DNA replication. The origins of replication of Φ29 DNA are located at the ends of the linear genome. Progression of the two replication forks would generate positive supercoiling ahead due to DNA unwinding that would greatly impair replication if DNA were not allowed to rotate freely. Thus, in a topologically restricted DNA, gyrase would be required for efficient replication. Therefore, we added novobiocin or nalidixic acid 30 min post-infection, once phage DNA replication had started, and measured DNA synthesis. Samples were taken 40 and 80 min post-infection and DNA extracted and analyzed by agarose gel electrophoresis (Figure 2A). Using real-time PCR we also

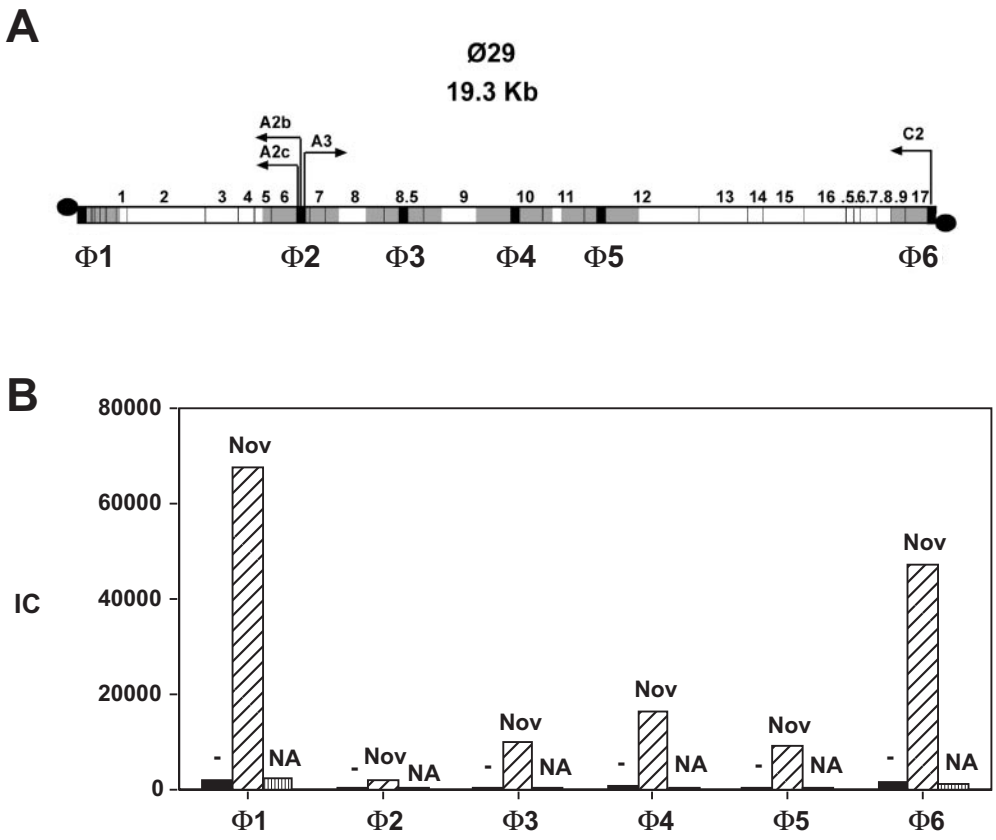

Figure 1. Effect of novobiocin and nalidixic acid in protein p6 binding to Φ29 DNA. (**A**) Genomic location of the Φ29 DNA regions analyzed for protein p6 binding. The positions of the genes, numbered 1 to 17, are indicated, .5 to .9 stands for genes 16.5 to 16.9. The 5′-bound terminal protein is depicted as a black circle. The arrows point the direction of transcription: early promoters C2, A2b and A2c transcribe leftwards and late promoter A3 rightwards. Six Φ29 DNA regions, named Φ1 to Φ6, were analyzed. Regions Φ1 and Φ6 correspond to the left and right Φ29 DNA ends, respectively; Φ6 also comprises early promoter C2. Φ2 includes the central transcriptional control region, with promoters A2b, A2c and A3. The analyzed regions include the PCR-amplified sequences, ∼300 bp long (black rectangles), and the flanking ∼450 bp (gray), as the average size of DNA after sonication is ∼750 bp. The amplified sequences were purified and used for fluorescence quenching assays (Figures 4 and 5). These DNA fragments were named L (left DNA end, comprised in region Φ1), 5.1 (comprised in Φ2), 7.4 (comprised in Φ3), 9.7 (comprised in Φ4), 11.7 (comprised in Φ5) and R (right DNA end, comprised in Φ6). (**B**) Protein p6 binding to Φ29 DNA regions. *B.subtilis* cells were grown, infected with Φ29 *sus14* (1242) and, after 20 min, the untreated aliquot (−) was crosslinked and processed as described in Materials and Methods; other two aliquots were treated with 34 μg/ml chloramphenicol together with 500 μg/ml novobiocin (Nov) or nalidixic acid (NA), and crosslinked 10 min later. Protein p6 binding is expressed as immunoprecipitation coefficient (IC, see Materials and Methods). IC values for each region are the following (−, Nov, NA). Φ1: 1935, 67448, 2320; Φ2: 230, 1760, 105; Φ3: 344, 9753, 151; Φ4: 458, 16059, 254; Φ5: 392, 9063, 238; Φ6: 1369, 46812, 915.

quantified accurately the amount of DNA from the left Φ29 DNA terminus (Figure 2B), shown in black in Figure 1A. Both stained gels and PCR analysis clearly indicate that the two inhibitors, especially novobiocin, already produce a significant impairment in DNA replication 10 min after their addition. Altogether these results indicate that the Φ29 genome is topologically constrained *in vivo* and, on the other hand, that gyrase is the first host protein shown to participate in Φ29 DNA replication.

Protein p6 binding to Φ29 DNA ends cloned in *E.coli*

The enhanced binding of p6 to regions Φ1 and Φ6, which contain the Φ29 DNA ends, could be due to the presence of independent topological domains in Φ29 DNA and/or to the presence of preferential binding sequences. To discriminate between these two possibilities we analyzed p6 binding *in vivo* to different Φ29 DNA regions in the same topological environment. For this, we cloned the left (L) or right (R) Φ29 DNA ends in plasmid pACYC184 at the region denominated P1 (see Figure 3A), and transformed a p6-producing *E.coli* strain. These inserts basically correspond to the amplified sequences of region Φ1 (L) and Φ6 (R). We also measured p6 binding to a concatemeric sequence (C) for which footprinting assays showed a preferential p6 binding *in vitro* (27). This concatemer contains 12 repetitions of a 24 bp sequence that would theoretically favor the formation of the p6-DNA complex (38), according to its predicted anisotropic bendability based on the algorithm developed by Travers and coworkers (52). As control, we used the pACYC184 plasmid with an insert of similar size of a non-related DNA sequence, a fragment of *E.coli* aspartate oxidase gene (AO). As internal control in every construction we measured p6 binding to a region, P2, of similar size located at the opposite site (see Figure 3A).

As Figure 3B shows, p6 binding for the concatemeric region (C) is 1.5- and 1.8-fold higher than for the left (L) and right (R) Φ29 DNA ends, respectively, and over 5-fold higher than for a non-Φ29 DNA sequence (AO). Binding to region P2 was similar in all cases, being slightly lower when binding to the corresponding region P1 was higher; as p6 restrains

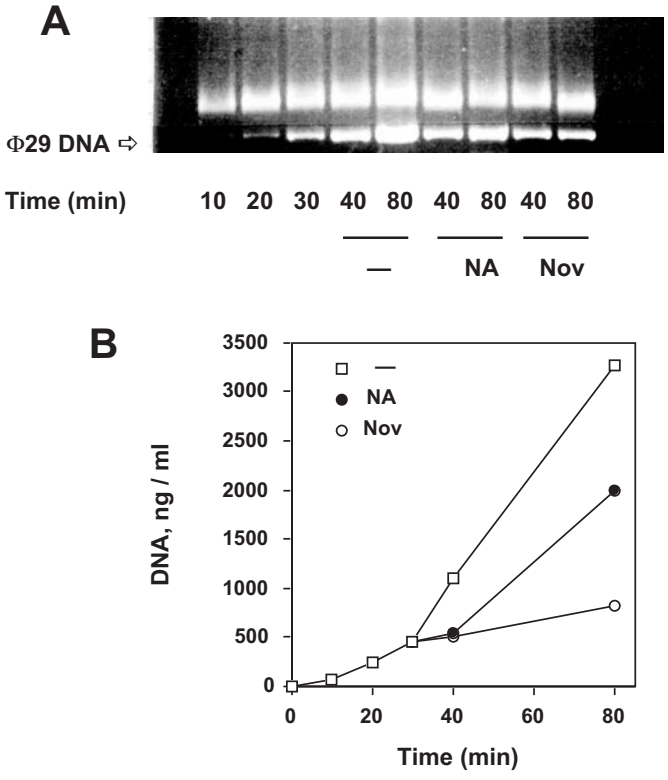

Figure 2. Effect of novobiocin and nalidixic acid on Φ29 DNA replication. *B.subtilis* cells were infected with Φ29 *sus14* (1242) and 30 min later the culture was divided into three aliquots and further grown in the presence of novobiocin (Nov), nalidixic acid (NA) (500 μg/ml each) or none (–). Aliquots were taken at the indicated times after infection, and the DNA was purified by phenol extraction and ethanol precipitation. (**A**) Agarose gel electrophoresis showing viral (lower band) and chromosomal DNA (upper band). (**B**) Amount of Φ29 DNA calculated by real time PCR of the left terminal sequence (259 bp). The data are expressed as nanograms of full-length Φ29 DNA per milliliter of culture.

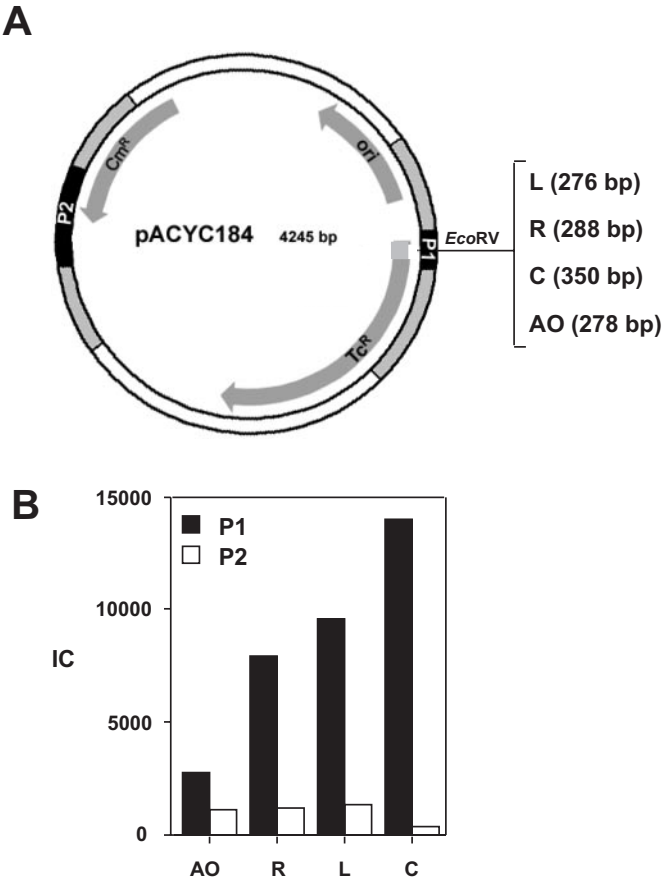

Figure 3. Protein p6 binding to DNA regions cloned in plasmid pACYC184. (**A**) Genetic map of plasmid pACYC184, indicating the EcoRV restriction site in region P1 (100 bp) in which the following sequences were inserted: Φ29 DNA left (L) and right (R) termini, a concatemer formed by 12 tandem repeats of a 24 bp p6 preferential binding sequence (C, see text for details) and an *E.coli* aspartate oxidase gene fragment (AO). The amplified sequences, P1 and P2, are depicted in black, and the DNA regions analyzed for p6 binding are shown in gray. Plasmid origin of replication and chloramphenicol and tetracycline resistance genes are also shown. (**B**) Protein p6 binding to DNA regions. Protein p6-producing *E.coli* cells were transformed with each of the four recombinant plasmids described in (A). The four strains were grown to $\sim 10^8$ cells/ml, 500 μg/ml novobiocin was added to increase p6 binding sensitivity, and after 10 min, cells were crosslinked and processed as described in Materials and Methods. Protein p6 binding is expressed as immunoprecipitation coefficient (IC, see Materials and Methods). IC values of regions P1 and P2 for the following inserts were, respectively, L, 9530 and 1289; R, 7890 and 1139; C, 13978 and 345; and AO, 2724 and 1103.

positive supercoiling, binding to high affinity sequences could originate compensatory negative supercoils along the free DNA, impairing further p6 binding (28). In conclusion, the higher affinity of p6 for regions Φ1 and Φ6 in Φ29-infected cells could be explained by the existence of nucleotide sequences that favor the formation of the nucleoprotein complex.

Protein p6 binding *in vitro* to Φ29 DNA sequences

To further investigate the role of the nucleotide sequence in protein p6 binding, we performed *in vitro* p6 binding assays using tryptophan fluorescence quenching, which allows calculation of the binding constant for a given DNA. We assayed all the amplified sequences (fragments ranging from 212 to 366 bp in length) from the six Φ29 DNA regions, Φ1 to Φ6, analyzed *in vivo* (see Figure 1A). It is very important to note that the p6 binding data *in vivo* (Figure 1B) correspond not only to the amplified sequence (in black in Figure 1A), but to the whole immunoprecipitated region (in gray in Figure 1A). Therefore, although correlated, the *in vivo* and *in vitro* data are not directly comparable. Thus, to avoid any confusion, we named the Φ29 DNA fragments according to their coordinates (in kb): 5.1 from region Φ2, 7.4 from region Φ3, 9.7 from region Φ4 and 11.7 from region Φ5. L and R stand for the left and right DNA termini, from regions Φ1 and Φ6, respectively.

To determine the effective binding constant (K_{eff}) values for the different DNA fragments we performed direct titration experiments (45,46) in which increasing amounts of p6 were added to 10 μM (bp) of the six fragments, L, 5.1, 7.4, 9.7, 11.7 or R (Figure 4A). At low protein concentration fluorescence values follow a straight line whose slope corresponds to the free protein. At a given concentration p6 begins to bind DNA, fluorescence is quenched and therefore the slope decreases. The inset of Figure 4A shows, enlarged, the p6 binding in the range 0.7–1.7 μM. Finally, when the protein saturates DNA, the initial slope is recovered, as the

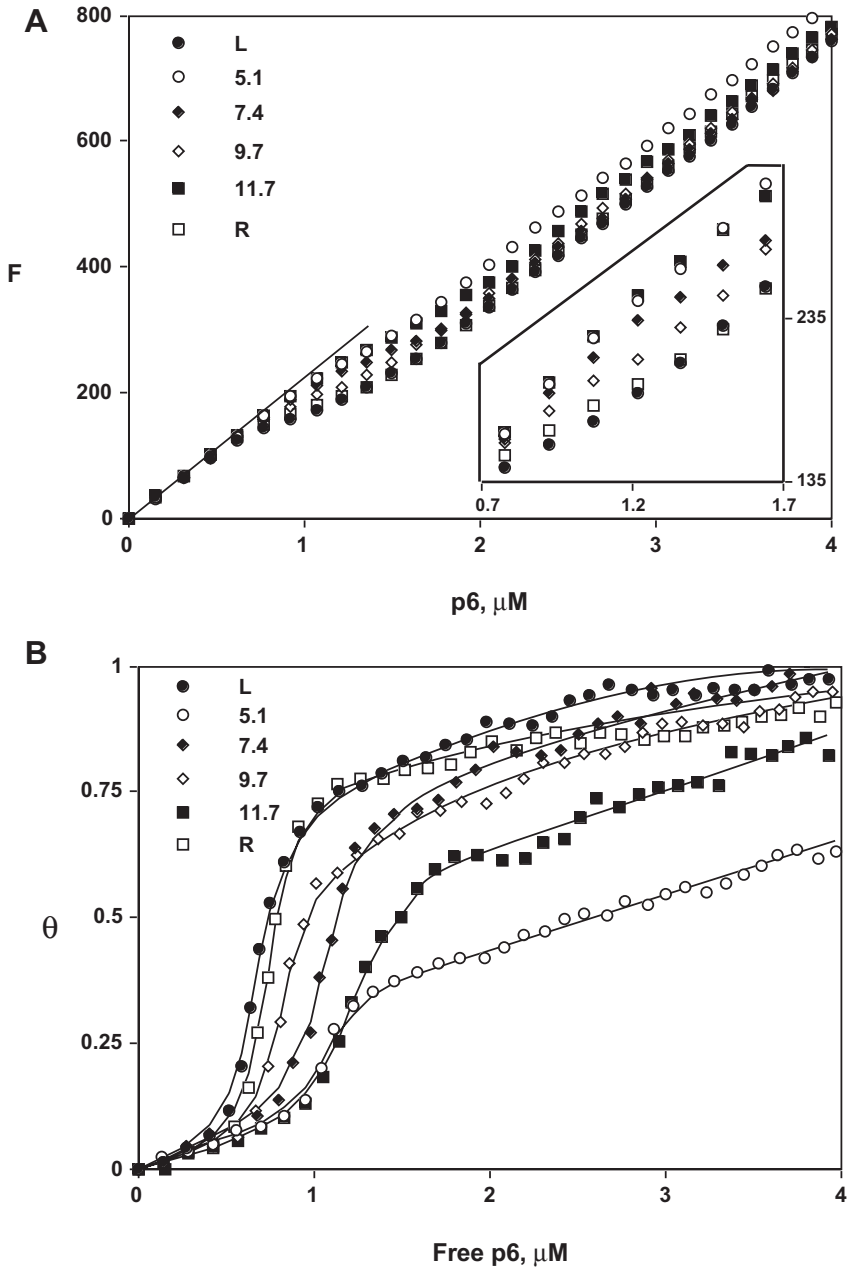

Figure 4. Protein p6 binding to Φ29 DNA sequences measured by fluorescence quenching. (**A**) Direct titration of p6 binding to the following Φ29 DNA fragments: L (259 bp), 5.1 (363 bp), 7.4 (237 bp), 9.7 (313 bp), 11.7 (212 bp) and R (298 bp). L and R stand for left and right Φ29 DNA ends, respectively, 5.1 to 11.7 correspond to the genome coordinates of the center of the fragments, and they are shown in black in Figure 1A. Therefore, L, 5.1, 7.4, 9.7, 11.7 and R are comprised in regions Φ1 to Φ6, respectively. Protein p6 was added to 10 μM DNA (in bp), and fluorescence measured continuously. The inset shows, enlarged, the plot in the 0.7–1.7 μM p6 range. (**B**) Graphical estimation of the K_{eff} of p6 for each fragment, in a plot of the saturation fraction (θ) versus concentration of free p6. These values are for a single representative experiment.

fluorescence values correspond again to the free protein. Therefore, the affinity of p6 for the DNA fragments can be easily compared from these graphs. Figure 4A shows that fragments R and, particularly, L have the highest affinity: p6 starts to bind at a lower concentration, the slope of the binding phase is the lowest and saturation is rapidly reached. Next follow the affinities for 9.7 and 7.4 and then 11.4, which only approaches saturation at high p6 concentrations. Finally, p6 binds with the lowest affinity to 5.1 and does not reach saturation at the highest protein concentration tested.

We computer-fitted the values of the titrations to K_{eff} values (see Materials and Methods) for each DNA in terms of the previously calculated value of maximal quenching [$Q_{max} = 0.84$, (28)], the molar fluorescence of the free protein ($f_A = 231\ \mu M^{-1}$) and the binding site size of a protein p6 monomer [$n = 12$, (26)]. The values of the K_{eff} (in M^{-1}) are as follows. L: 13.6×10^5; 5.1: 4.0×10^5; 7.4: 8.0×10^5; 9.7: 10.0×10^5; 11.7: 6.0×10^5 and R: 12.4×10^5. We have also performed a graphical approximation to the K_{eff} values (Figure 4B). In a plot of the saturation fraction (θ) against

the free protein, which is derived from the direct titration data, the inverse of $[p6]_{free}$ when 50% of the DNA is bound to protein is approximately the value of K_{eff}. The values obtained (L: 13.5×10^5; 5.1: 4.0×10^5; 7.4: 8.9×10^5; 9.7: 10.4×10^5; 11.7: 6.7×10^5 and R: 12.5×10^5) are close to those calculated directly from Figure 4A.

As stated previously, p6 preferential binding to Φ29 DNA terminal regions could be due to the presence of sequences with anisotropic bendability that favors the formation of the nucleoprotein complex. We have just shown that p6 binding *in vivo* to a concatemer of 12 repetitions of such a sequence, named fragment C, is higher than that to Φ29 DNA ends (Figure 3). In addition, p6 binding *in vitro* to fragment C was measured by fluorescence quenching and directly compared with binding to L, the Φ29 fragment with highest affinity. The lowest binding affinity corresponded to fragment 5.1, which contains an intrinsic DNA curvature (53,54), whose rigid structure could impair p6 binding. To test this hypothesis, we measured p6 affinity for two overlapping fragments in which the 50 bp curved tract was excluded (Figure 5A). These fragments, named 4.9 and 5.3 after their genome coordinates, are similar in size to fragment 5.1. Figure 5B shows a direct titration of p6 by fragments C, 4.9 and 5.3, along with fragments L and 5.1 for comparison. It is clear that p6 affinity for fragment C is higher than for any other fragment. The calculated K_{eff} value is 26.2×10^5, nearly twice that for L (13.5×10^5). As for fragments 4.9 and 5.3, their K_{eff} values are 9.4×10^5 and 8.8×10^5, respectively, more than twice that of fragment 5.1 (4.0×10^5). Figure 5C shows a graphical approximation to the constants, as in Figure 4B. Again, the K_{eff} values are very similar, 25.0×10^5 for fragment C, 9.8×10^5 for 4.9, and 8.8×10^5 for 5.3. These results strongly suggest that the structural properties of a given DNA sequence may determine the p6 binding affinity.

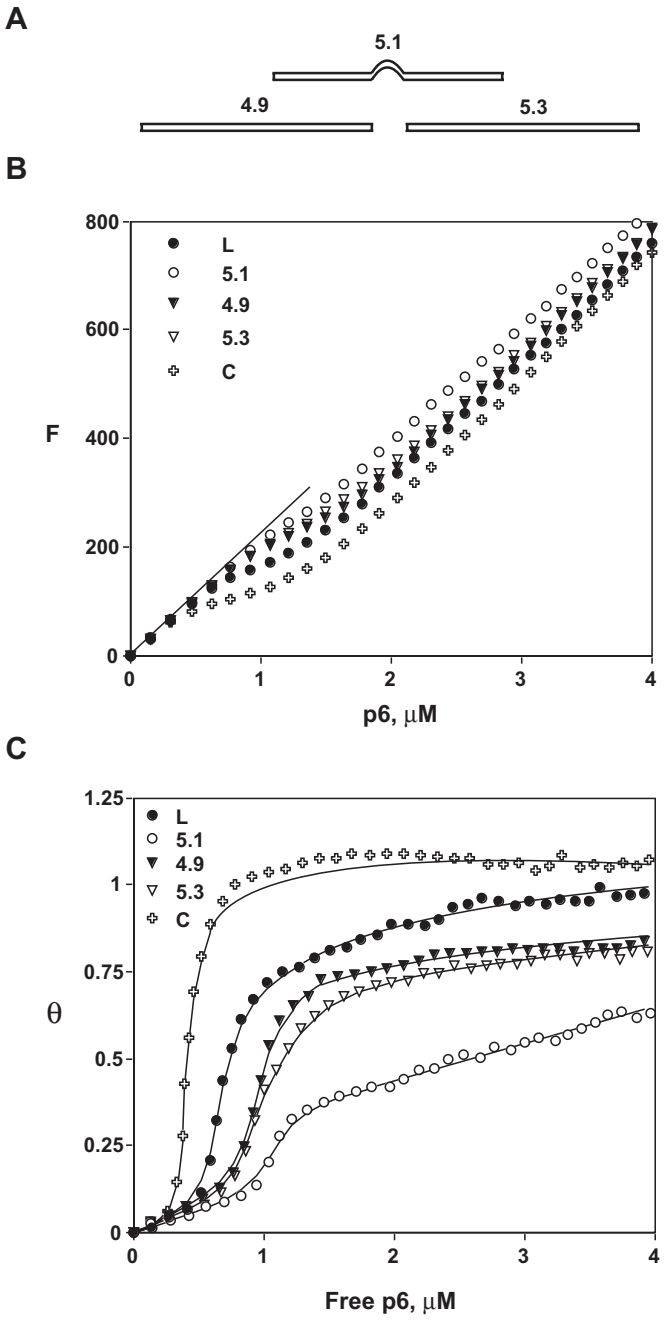

Figure 5. Protein p6 binding to DNA fragments measured by fluorescence quenching. (**A**) Diagram of Φ29 DNA fragments 4.9, 5.1 and 5.3, showing the position of the curved region of fragment 5.1. Fragments 4.9 and 5.3 overlap fragment 5.1 but lack the intrinsic curvature; 4.9 and 5.3 stand for the Φ29 DNA coordinates of the center of the fragment. (**B**) Direct titration of p6 binding to the following DNA fragments: L (259 bp) and 5.1 (363 bp) are the Φ29 DNA fragments described in Figure 4A; 4.9 (335 bp) and 5.3 (328 bp) are the fragments shown in (A), and C (350 bp) is a 12 tandem repeats concatemer of a 24 bp sequence of p6 preferential binding. (**C**) Graphical estimation of the K_{eff} values of p6 for each fragment, in a plot of the saturation fraction (θ) versus concentration of free p6.

DISCUSSION

In addition to its well characterized function in DNA replication and transcriptional control (55), protein p6 binds *in vivo* to most, if not all, of the Φ29 DNA (28), which strongly suggests a role in the global organization and compaction of the viral genome. Its small size and abundance in infected cells [∼700 000 copies per cell, (29)] are features expected for a protein with an architectural role. Protein p6 does not recognize a specific DNA sequence; however, in infected cells it can discriminate viral from bacterial DNA, as binding to plasmid DNA is negligible (28). Binding to plasmid DNA *in vivo* increases dramatically upon addition of novobiocin, which inhibits gyrase, producing a decrease in negative supercoiling. The p6 supercoiling-dependent binding was confirmed and quantified by *in vitro* studies (28) and it is consistent with the ability of p6 to restrain positive supercoiling (27,56). Therefore, the specificity of p6 for Φ29 DNA is most probably based on its preferential binding to DNAs with lower negative superhelicity, as is presumably the case of the non-covalently closed Φ29 genome with respect to host DNA. In this work, we demonstrate that Φ29 DNA, although it has a terminal protein covalently linked to the ends, and therefore is not covalently closed, is topologically constrained. Evidence supporting Φ29 DNA topological restriction is 2-fold. First there is the nearly 30-fold increase of p6 binding upon novobiocin treatment, as was described for plasmid DNA (28). Novobiocin inhibits gyrase, producing a loss of negative supercoiling; if Φ29 DNA were unconstrained, novobiocin should have no effect.

In contrast, nalidixic acid, which also inhibits gyrase but produces no topological change (51) did not increase p6 binding. The second piece of evidence for topological restriction is the inhibition of Φ29 DNA replication by the gyrase inhibitors, novobiocin and nalidixic acid. The higher inhibition by novobiocin could be due to the increase of p6 binding: an excess of positive supercoiling would further hinder strand separation during replication. Therefore, gyrase is required for Φ29 DNA replication, being the first host protein shown to be involved in this process.

This topological constraint is most probably due to membrane attachment (57), presumably through the terminal proteins, which has been shown to have intrinsic affinity for the membrane (58). In addition, two membrane-associated viral proteins involved in Φ29 DNA replication are probably implicated in this attachment, p16.7 (59) and p1, the latter proposed to be a component of a scaffold for the assembly of the viral DNA replication machinery (60).

The topological constraint of Φ29 DNA may be essential to understanding the functions of protein p6, namely DNA replication and the switch from early to late transcription. More interestingly, other functions for p6 could be envisaged: for example, it could play a role in segregation of the viral DNA progeny. It has been shown that throughout the infective cycle Φ29 DNA undergoes a dynamic relocalization, spreading into multiple replication foci (61). The protein p6-induced positive supercoiling, leading to DNA compaction, may be essential for this process in a way similar to that proposed for bacterial chromosome partitioning (62). In *E.coli* this partitioning requires MukB protein, which is known to be involved, like protein p6, in DNA condensation and supercoiling (63). In *B.subtilis*, MukB equivalent Smc protein is also involved in chromosome condensation and partitioning through supercoiling (64); a eukaryotic SMC, condensin 13S, restrains toroidal positive supercoiling *in vitro* (65), just as protein p6 does. Thus, protein p6 could be functionally equivalent to Smc proteins for the viral DNA segregation process.

Once it has been determined that the Φ29 genome is constrained, the simplest model would assume a single topological domain in Φ29 DNA. However, the fact that p6 binds to DNA regions with different affinities could be explained by the existence of independent topological domains. The evidence shown in this paper argues against this hypothesis. The p6 binding preferences for different regions remained unchanged after novobiocin addition (Figure 1B), and are also maintained *in vitro* (Figure 4A and B). In Figure 6 we show the data for p6 binding to Φ29 DNA *in vivo* and *in vitro* normalized to those of region Φ1 or fragment L, respectively. Although the differences of p6 binding *in vitro* among the regions are less pronounced, specifically in terms of terminal versus central regions, they are qualitatively analogous to the corresponding Φ29 DNA regions *in vivo*.

The preferential binding to the DNA ends is probably due to the presence of sequences with bendability properties that favor the formation of the p6–DNA complex, in accordance with previously published predictions (38). In fact, the 24 bp sequence of the concatemer used in our studies is highly flexible and is kinked about 90° (66). This preferential binding is probably related to the p6 activation of replication origins at both DNA ends (20,21). Another important role of p6 at the right DNA end is switching off the very early promoter C2,

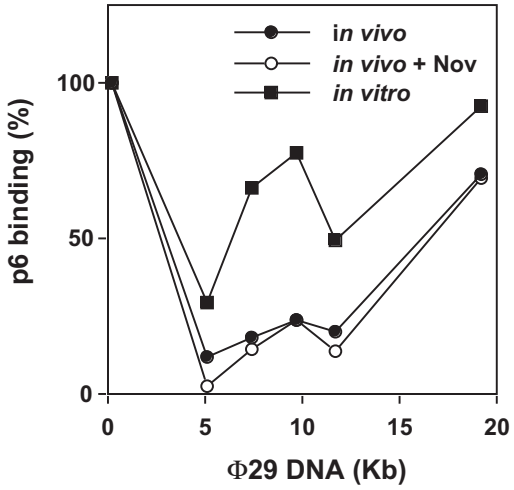

Figure 6. Comparison of p6 binding to Φ29 DNA regions *in vivo* and *in vitro*. IC values for *in vivo* p6 binding to regions Φ1 to Φ6, with or without novobiocin (Nov), are from Figure 1B, and were normalized to those of region Φ1. K_{eff} values for *in vitro* p6 binding to fragments L to R are from Figure 4A, and were normalized to that of fragment L. The relative binding values were plotted versus their position in Φ29 DNA.

which controls the expression of proteins involved in phage DNA injection (67). A high p6 affinity for this region is necessary to ensure a rapid repression of the promoter at the beginning of the infective cycle, when the p6 concentration is still low.

The particularly low p6 affinity for the transcription control region, comprised in fragment 5.1 *in vitro* and region Φ2 *in vivo*, seems to be due to the presence of an intrinsic curvature, located at the protein p4 binding site at promoter A2b (53,54). The rigidity of this sequence could impair the formation of the nucleoprotein complex, which, as stated above, requires bendable sequences. In fact, we show that protein p6 binding to partially overlapping DNA fragments that lack the intrinsic curvature is much higher, with affinity values similar to those of the other internal Φ29 DNA fragments. The low p6 binding to region Φ2 *in vivo* may be essential for the correct timing of the transcription program of the phage. Protein p6 increases binding of p4 to its cognate site at promoter A2b (25), which induces its repression and the activation of late promoter A3 (68,69). Given the high synthesis rate of protein p6, its affinity for this region must be kept low to prevent a premature switching from early to late transcription, which would give rise to a shorter infective cycle and a low phage production.

In conclusion, we show that protein p6 binding to Φ29 DNA *in vivo* is enhanced when cells are treated with novobiocin, which decreases negative supercoiling, but not when treated with nalidixic acid, which does not change topology. However, both novobiocin and nalidixic acid impair viral DNA replication, indicating the involvement of gyrase in this process. Both results lead to the conclusion that the Φ29 genome is topologically constrained *in vivo*. We also show that protein p6 binding is favored by nucleotide sequences with precise bendability properties, and impaired by rigid DNA tracts. The local variations of p6 affinity may be very important for processes such as DNA replication and regulation of transcription.

ACKNOWLEDGEMENTS

We are indebted to Dr M. G. Mateu for assistance with the fluorescence experiments. We are grateful to Dr A. Bravo for providing *B.subtilis* strain 110NA pPR55ow6, and L. Villar for purified Φ29 DNA. This work was supported by research grants 2R01 GM27242-24 from the National Institutes of Health, BMC2002-03818 from the Ministry of Science and Technology and by an Institutional grant from the Fundación Ramón Areces to the Centro de Biología Molecular 'Severo Ochoa'. V.G.-H. was a postdoctoral fellow of the Comunidad Autónoma de Madrid and M.A. was a predoctoral fellow of the Ministry of Science and Technology.

REFERENCES

1. Haushalter,K.A. and Kadonaga,J.T. (2003) Chromatin assembly by DNA-translocating motors. *Nature Rev. Mol. Cell Biol.*, **4**, 613–620.
2. Fischle,W., Wang,Y. and Allis,C.D. (2003) Histone and chromatin cross-talk. *Curr. Opin. Cell Biol.*, **15**, 172–183.
3. Thomas,J.O. and Travers,A.A. (2001) HMG1 and 2, and related 'architectural' DNA-binding proteins. *Trends Biochem. Sci.*, **26**, 167–174.
4. Travers,A.A. (2003) Priming the nucleosome: a role for HMGB proteins? *EMBO Rep.*, **4**, 131–136.
5. Hirano,T. (1999) SMC-mediated chromosome mechanics: a conserved scheme from bacteria to vertebrates? *Genes Dev.*, **13**, 11–19.
6. Strunnikov,A.V. and Jessberger,R. (1999) Structural maintenance of chromosomes (SMC) proteins: conserved molecular properties for multiple biological functions. *Eur. J. Biochem.*, **263**, 6–13.
7. Drlica,K. and Rouvière-Yaniv,J. (1987) Histone-like proteins of bacteria. *Microbiol. Rev.*, **51**, 301–319.
8. Hayat,M.A. and Mancarella,D.A. (1995) Nucleoid proteins. *Micron*, **26**, 461–480.
9. Azam,T.A., Iwata,A., Nishimura,A., Ueda,S. and Ishihama,A. (1999) Growth phase-dependent variation in protein composition of the *Escherichia coli* nucleoid. *J. Bacteriol.*, **181**, 6361–6370.
10. Azam,T.A., Hiraga,S. and Ishihama,A. (2000) Two types of localization of the DNA-binding proteins within the *Escherichia coli* nucleoid. *Genes Cells*, **5**, 613–626.
11. Niki,H., Imamura,R., Kitaoka,M., Yamanaka,K., Ogura,T. and Hiraga,S. (1992) *E.coli* MukB protein involved in chromosome partition forms a homodimer with a rod-and-hinge structure having DNA binding and ATP/GTP binding activities. *EMBO J.*, **11**, 5101–5109.
12. Kohler,P. and Marahiel,M.A. (1997) Association of the histone-like protein HBsu with the nucleoid of *Bacillus subtilis*. *J. Bacteriol.*, **179**, 2060–2064.
13. Tapias,A., López,G. and Ayora,S. (2000) *Bacillus subtilis* LrpC is a sequence-independent DNA-binding and DNA-bending protein which bridges DNA. *Nucleic Acids Res.*, **28**, 552–559.
14. Exley,R., Zouine,M., Pernelle,J.J., Beloin,C., Le Hegarat,F. and Deneubourg,A.M. (2001) A possible role for L24 of *Bacillus subtilis* in nucleoid organization and segregation. *Biochimie*, **83**, 269–275.
15. Graumann,P.L. (2001) SMC proteins in bacteria: condensation motors for chromosome segregation? *Biochimie* **83**, 53–59.
16. Mascarenhas,J., Soppa,J., Strunnikov,A.V. and Graumann,P.L. (2002) Cell cycle-dependent localization of two novel prokaryotic chromosome segregation and condensation proteins in *Bacillus subtilis* that interact with SMC protein. *EMBO J.*, **21**, 3108–3118.
17. Soppa,J., Kobayashi,K., Noirot-Gros,M.-F., Oesterhelt,D., Ehrlich,S.D., Dervyn,E., Ogasawara,N. and Moriya,S. (2002) Discovery of two new families of proteins, which are proposed to interact with prokaryotic SMC proteins, and characterization of the *Bacillus subtilis* family members Ypu and YpuH. *Mol. Microbiol.*, **45**, 59–71.
18. Schachtele,C.F., Reilly B.E., De Sain C.V., Whittington M.O. and Anderson D.L. (1973) Selective replication of bacteriophage Φ29 deoxyribonucleic acid in 6-(p-hydroxyphenylazo)-uracil-treated *Bacillus subtilis*. *J. Virol.*, **11**, 153–155.
19. Carrascosa,J.L., Camacho,A., Moreno,F., Jiménez,F., Mellado,R.P., Viñuela,E. and Salas,M. (1976) *Bacillus subtilis* phage Φ29: characterization of gene products and functions. *Eur. J. Biochem.*, **66**, 229–241.
20. Pastrana,R., Lázaro,J.M., Blanco,L., García,J.A., Méndez,E. and Salas,M. (1985) Overproduction of protein p6 of *Bacillus subtilis* phage Φ29: role in the initiation of DNA replication. *Nucleic Acids Res.*, **13**, 3083–3100.
21. Blanco,L., Gutiérrez,J., Lázaro,J.M., Bernad,A. and Salas,M. (1986) Replication of phage Φ29 DNA *in vitro*: role of the viral protein p6 in initiation and elongation. *Nucleic Acids Res.*, **14**, 4923–4937.
22. Whiteley,H.R., Ramey,W.D., Spiegelman,G.B. and Holder,R.D. (1986) Modulation of *in vivo* and *in vitro* transcription of bacteriophage Φ29 early genes. *Virology*, **155**, 392–401.
23. Barthelemy,I., Mellado,R.P. and Salas,M. (1989) *In vitro* transcription of bacteriophage Φ29 DNA: inhibition of early promoters by the viral replication protein p6. *J. Virol.*, **63**, 460–462.
24. Camacho,A. and Salas,M. (2001) Repression of bacteriophage Φ29 early promoter C2 by viral protein p6 is due to impairment of closed complex. *J. Biol. Chem.*, **276**, 28927–28932.
25. Elías-Arnanz,M. and Salas,M. (1999) Functional interactions between a phage histone-like protein and a transcriptional factor in regulation of Φ29 early-late transcriptional switch. *Genes Dev.*, **13**, 2502–2513.
26. Serrano,M., Salas,M. and Hermoso,J.M. (1990) A novel nucleoprotein complex at a replication origin. *Science*, **248**, 1012–1016.
27. Serrano,M., Gutiérrez,C., Salas,M. and Hermoso,J.M. (1993) Superhelical path of the DNA in the nucleoprotein complex that activates the initiation of phage Φ29 DNA replication. *J. Mol. Biol.*, **230**, 248–259.
28. González-Huici,V., Salas,M. and Hermoso J.M. (2004) Genome wide, supercoiling-dependent, *in vivo* binding of a viral protein involved in DNA replication and transcriptional control. *Nucleic Acids Res.*, **32**, 2306–2314.
29. Abril,A.M., Salas,M., Andreu,J.M., Hermoso,J.M. and Rivas,G. (1997) Phage Φ29 protein p6 is in a monomer–dimer equilibrium that shifts to higher association states at the millimolar concentrations found *in vivo*. *Biochemistry*, **36**, 11901–11908.
30. McLeod,S.M. and Johnson,R.C. (2001) Control of transcription by nucleoid proteins. *Curr. Opin. Microbiol.*, **4**, 152–159.
31. Dorman,C.J. and Deighan,P. (2003) Regulation of gene expression by histone-like proteins in bacteria. *Curr. Opin. Genet. Dev.*, **13**, 179–184.
32. Hommais,F., Krin,E., Laurent-Winter,C., Soutourina,O., Malpertuy,A., LeCaer,J.P., Danchin,A. and Bertin,P. (2001) Large-scale monitoring of pleiotropic regulation of gene expression by the prokaryotic nucleoid-associated protein, H-NS. *Mol. Microbiol.*, **40**, 20–36.
33. Schroder,O. and Wagner,R. (2002) The bacterial regulatory protein H-NS—a versatile modulator of nucleic acid structures. *Biol. Chem.*, **383**, 945–960.
34. Hwang,D.S. and Kornberg,A. (1992) Opening of the replication origin of *Escherichia coli* by DnaA protein with protein HU or IHF. *J. Biol. Chem.*, **267**, 23083–23086.
35. Ryan,V.T., Grimwade,J.E., Camara,J.E., Crooke,E. and Leonard,A.C. (2004) *Escherichia coli* prereplication complex assembly is regulated by dynamic interplay among Fis, IHF and DnaA. *Mol. Microbiol.*, **51**, 1347–1359.
36. Pettijohn,D.E. and Pfenninger,O. (1980) Supercoils in prokaryotic DNA restrained *in vivo*. *Proc. Natl Acad. Sci. USA*, **77**, 1331–1335.
37. Sinden,R.R. and Pettijohn,D.E. (1981) Chromosomes in living *Escherichia coli* cells are segregated into domains of supercoiling. *Proc. Natl Acad. Sci. USA*, **78**, 224–228.
38. Serrano,M., Gutiérrez,J., Prieto,I., Hermoso,J.M. and Salas,M. (1989) Signals at the bacteriophage Φ29 DNA replication origins required for protein p6 binding and activity. *EMBO J.*, **8**, 1879–1885.
39. Moreno,F., Camacho,A., Viñuela,E. and Salas,M. (1974) Supressor-sensitive mutants and genetic map of *Bacillus subtilis* bacteriophage Φ29. *Virology*, **62**, 1–16.
40. Bravo,A., Hermoso,J.M. and Salas,M. (1994) A genetic approach to the identification of functional amino acids in protein p6 of *Bacillus subtilis* phage Φ29. *Mol. Gen. Genet.*, **245**, 529–536.
41. Jiménez,F., Camacho,A., De La Torre,J., Viñuela,E. and Salas,M. (1977) Assembly of *Bacillus subtilis* phage Φ29. 2. Mutants in the cistrons coding for the non-structural proteins. *Eur. J. Biochem.*, **73**, 57–72.
42. Inciarte,M.R., Lázaro,J.M., Salas,M. and Viñuela,E. (1976) Physical map of bacteriophage Φ29 DNA. *Virology*, **74**, 314–323.

43. González-Huici,V., Salas,M. and Hermoso,J.M. (2000) Sequence requirements for protein-primed initiation and elongation of phage Φ29 DNA replication. *J. Biol. Chem.*, **275**, 40547–40553.
44. Lin,D.C.H. and Grossman,A.D. (1998) Identification and characterization of a bacterial chromosome partitioning site. *Cell*, **92**, 675–685.
45. Alma,N.C., Harmsen,B.J., de Jong,E.A., Ven,J. and Hilbers,C.W. (1983) Fluorescence studies of the complex formation between the gene 5 protein of bacteriophage M13 and polynucleotides. *J. Mol. Biol.*, **163**, 47–62.
46. Schwarz,G. and Watanabe,F. (1983) Thermodynamics and kinetics of co-operative protein-nucleic acid binding. I. General aspects of analysis of data. *J. Mol. Biol.*, **163**, 467–484.
47. McGhee J.D. and von Hippel,P.H. (1974) Theoretical aspects of DNA-protein interactions: co-operative and non-co-operative binding of large ligands to a one-dimensional homogeneous lattice. *J. Mol. Biol.*, **86**, 469–489.
48. Soengas,M.S., Esteban,J.A., Salas,M. and Gutiérrez,C. (1994) Complex formation between phage Φ29 single-stranded DNA binding protein and DNA. *J. Mol. Biol.*, **239**, 213–226.
49. Kowalczykowski,S.C., Paul,L.S., Lonberg,N., Newport,J.W., McSwiggen,J.A. and von Hippel,P.H. (1986) Cooperative and noncooperative binding of protein ligands to nucleic acid lattices: experimental approaches to the determination of thermodynamic parameters. *Biochemistry*, **25**, 1226–1240.
50. Orlando,V. (2000) Mapping chromosomal proteins *in vivo* by formaldehyde-crosslinked-chromatin immunoprecipitation. *Trends Biochem. Sci.*, **25**, 99–104.
51. Osburne,M.S., Zavodny,S.M. and Peterson,G.A. (1988) Drug-induced relaxation of supercoiled plasmid DNA in *Bacillus subtilis* and induction of the SOS response. *J. Bacteriol.*, **170**, 442–445.
52. Satchwell,S.C., Drew,H.R. and Travers,A.A. (1986) Sequence periodicities in chicken nucleosome core DNA. *J. Mol. Biol.*, **191**, 659–675.
53. Barthelemy,I. and Salas,M. (1989) Characterization of a new prokaryotic transcriptional activator and its DNA recognition site. *J. Mol. Biol.*, **208**, 225–232.
54. Rojo,F., Zaballos,A. and Salas,M. (1990) Bend induced by the phage Φ29 transcriptional activator in the viral late promoter is required for activation. *J. Mol. Biol.*, **211**, 713–725.
55. Meijer,W.J.J., Horcajadas,J.A. and Salas,M. (2001) Φ29 family of phages. *Microbiol. Mol. Biol. Rev.*, **65**, 261–287.
56. Prieto,I., Serrano,M., Lázaro,J.,M., Salas,M. and Hermoso,J.M. (1988) Interaction of the bacteriophage ϕ 29 protein p6 with double-stranded DNA. *Proc. Natl Acad. Sci. USA*, **85**, 314–318.
57. Ivarie,R.D. and Pène,J.J. (1973) DNA replication in bacteriophage Φ29: the requirement of a viral-specific product for association of Φ29 DNA with the cell membrane of *Bacillus amyloliquefaciens*. *Virology*, **52**, 351–362.
58. Bravo,A. and Salas,M. (1997) Initiation of bacteriophage Φ29 DNA replication *in vivo*: Assembly of a membrane-associated multiprotein complex. *J. Mol. Biol.*, **269**, 102–112.
59. Meijer,W.J.J., Serna-Rico,A. and Salas,M. (2001) Characterization of the bacteriophage Φ29-encoded protein p16.7: a membrane protein involved in phage DNA replication. *Mol. Microbiol.*, **39**, 731–746.
60. Bravo,A. and Salas,M. (1998) Polymerization of bacteriophage Φ29 replication protein p1 into protofilament sheets. *EMBO J.*, **17**, 6096–6105.
61. Meijer,W.J.J., Lewis,P.J., Errington,J. and Salas,M. (2000) Dynamic relocalization of phage Φ29 DNA during replication and the role of the viral protein p16.7. *EMBO J.*, **19**, 4182–4190.
62. Holmes,V.F. and Cozzarelli,N.R. (2000) Closing the ring: links between SMC proteins and chromosome partitioning, condensation and supercoiling. *Proc. Natl Acad. Sci. USA*, **97**, 1322–1324.
63. Weitao,T., Nordstrom,K. and Dasgupta,S. (2000) *Escherichia coli* cell cycle control genes affect chromosome superhelicity. *EMBO Rep.*, **1**, 494–499.
64. Britton,R.A., Lin,D.C. and Grossman,A.D. (1998) Characterization of a prokaryotic SMC protein involved in chromosome partitioning. *Genes Dev.*, **12**, 1254–1259.
65. Kimura,K., Rybenkov,V.V., Crisona,N.J., Hirano,T. and Cozzarelli,N.R. (1999) 13S condensin actively reconfigures DNA by introducing global positive writhe: implications for chromosome condensation. *Cell*, **98**, 239–248.
66. Harrington,R.E. and Winicov,I. (1994) New concepts in protein-DNA recognition: sequence-directed DNA bending and flexibility. *Prog. Nucleic Acid Res. Mol. Biol.*, **47**, 195–270.
67. González-Huici,V., Salas,M. and Hermoso J.M. (2004) The push-pull mechanism of bacteriophage Φ29 DNA injection. *Mol. Microbiol.*, **52**, 529–540.
68. Salas,M. and Rojo,F. (1993) Replication and transcription of bacteriophage Φ29 DNA. In Hoch,J.A. and Losick,R. (eds), *Bacillus subtilis and other Gram-positive Bacteria: Biochemistry, Physiology, and Molecular Genetics*. American Society for Microbiology, Washington, DC, pp. 843–857.
69. Rojo,F., Mencia,M., Monsalve,M. and Salas,M. (1998) Transcription activation and repression by interaction of a regulator with the α subunit of RNA polymerase. *Prog. Nucleic Acid Res. Mol. Biol.*, **60**, 29–46.